Numerical Simulation of the Effect of Number of Runner Blades on a Cross-Flow Turbine Performance

Piter Harefa[1], Muhammad Agung Bramantya[1*], and Joko Waluyo[1]

[1] Department of Mechanical and Industrial Engineering, Faculty of Engineering, Universitas Gadjah Mada, Indonesia

Corresponding author's email: bramantya@mail.ugm.ac.id

Abstract. The utilization of renewable energy, particularly from hydropower, is still a developing field of research, and the optimal design for maximum efficiency remains a challenge to achieve. The objective of this study is to investigate the impact of the number of runner blades on the performance of a cross-flow turbine through computational fluid dynamics. The cross-flow turbine designed and experimentally tested by Sammartano et al. (2016) is used in simulation then modified impeller by changing the number of runner blades from 35 to 25 and 45. The simulation is conducted in a transient manner using a three-dimensional model and applied mesh motion method. The CFD simulation results indicate that the maximum efficiencies obtained using 25, 35 and 45 runner blades were 88.2%, 87.0% and 89.3% respectively. The impeller with 45 runner blades shows a more uniform velocity profile and a reduced exit angl. The pressure at the center and exit of the impeller is also lower, indicating a higher conversion of kinetic energy into rotational motion. Additionally, there is a reduction in turbulent kinetic energy, resulting in an enhanced output torque.

Keywords: Cross-flow turbine, Impeller, Runner blades, Computational fluid dynamics, Efficiency.

1 INTRODUCTION

Renewable energy, especially hydropower, plays a crucial role in addressing global energy needs. Hydropower is the largest source of renewable electricity worldwide, accounting for a significant portion of global renewable energy generation. It not only provides clean energy but also offers key grid services like energy storage, grid balancing, and flexible generation, complementing other renewables such as solar and wind when these sources are intermittent [1].

The significant progress has been made, with conventional hydropower growing by more than 75% in 2000-2021, reaching an installed capacity of over 1230 gigawatts (GW). Pumped storage hydropower (PSH) capacity, on the other hand, grew by over 50% in the same period, reaching 130 GW in 2021. Together, they account for over 50% of global renewable installed capacity [2].

Hydropower will have to play a crucial role in keeping the rise in global temperatures to 1.5 degrees Celsius (°C), providing power, flexibility and reliable support for power systems. To achieve this, however, hydropower's deployment pace will need to

M. A. Muflikhun et al. (eds.), *Proceedings of the 10th International Conference on Science and Technology (ICST 2024)*, Advances in Engineering Research 268,
https://doi.org/10.2991/978-94-6463-772-4_3

increase substantially, especially considering the projected increase in clean electricity demand owing to the decarbonisation of end-use sectors and a rapidly ageing hydropower fleet [3].

Hydropower is classified based on power generating capacity. One such type is the micro hydropower plant which has a range of power generating capacity of 5-100 kW [4-5]. This energy source is also widely found in remote areas where there are many waterways such as rivers, irrigation channels and process water treatment channels and wastewater treatment channels [6-7].

In the last few decades, the utilization of micro hydropower has been implemented in micro hydroelectric power plants (MHPP). One of its major components is the turbine. One type of turbine that is often used in micro hydropower plants is the cross-flow turbine (CFT). CFT is often used on sites with low head conditions and high-water discharge. It is more suitable and more cost-effective because of its simpler design and construction to be built at the power plant site. It also has relatively constant efficiency over a wide range of load or water discharge [8-11].

Research on cross flow turbines, especially regarding the design and its effect on turbine performance has been carried out experimentally. These studies have indicated that the performance of cross flow turbine depends on geometrical parameters. One of the important parameters is the number of runner blades (N_b).

In 1994, Desai and Aziz conducted experimental study and observed that there was an increase in efficiency from 64.1% to 74.5% by increasing runner of blades from 15 to 25 [12]. Sammartano et al. [7] and Sinagra et al. [13] also conducted experimental study by using 35 runner blades and obtained maximum efficiency 82.1%. In 2016, Sammartano also conducted experimental study and obtained maximum efficiency 80.6% using 35 runner blades [11].

From these experimental studies, this study focuses on investigating the effect of the number of runner blades on the efficiency of cross-flow turbines using computational fluid dynamic (CFD) method. Experimental study conducted by Sammartano et al. (2016) is used as reference for validation where cross flow turbine model has been designed using new formula. The model has also been experimentally tested with efficiencies of 75-80.6% using 35 runner blades. This is an interesting topic of this research because the effect of the number of runner blades used on turbine performance needs to be further analyzed and this can be done through a CFD-based numerical simulation process.

2 MATERIAL AND METHODS

2.1 Description of the Solvers

This study was conducted using a three-dimensional (3D) numerical method. Modelling begins with creating a 3D domain of a cross-flow turbine. The model refers to the experimental study conducted by Sammartano et al. [14] that consist of nozzle, impeller, casing and shaft. It is shown in Figure 1.

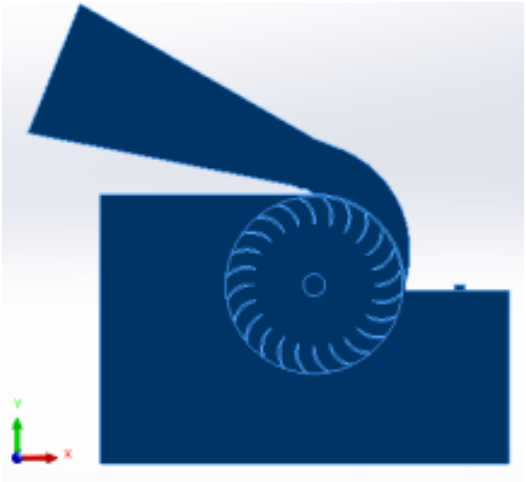

Fig. 1. CFT Model (Reference)

The design geometrical parameters used is designed by Sammartano in the previous study [11]. The impeller has a width of 139 mm and installed with 35 runner blades. Attack angle of the outlet nozzle velocity is 22°. The geometrical parameters shown in Figure 2 and the detail dimension of parameters shown in Table 1.

In the meshing process, the domain is divided into two physical sub-domains as shown in Figure 3. In more detail, the domain is divided into two main parts where the part is used for multizone meshing which is adapted to solving the case based on the mesh motion method. In modelling the turbine analysis system with the mesh motion method, the turbine is defined to have its own mesh with a rotational motion scheme according to the input angular velocity in the cell zone conditions. Meanwhile, the fluid is set as a flow in a fixed volume control. Multizone meshing method is used to control the cell quality in each part. In detail, the general meshing settings in each domain are carried out in accordance with Table 2.

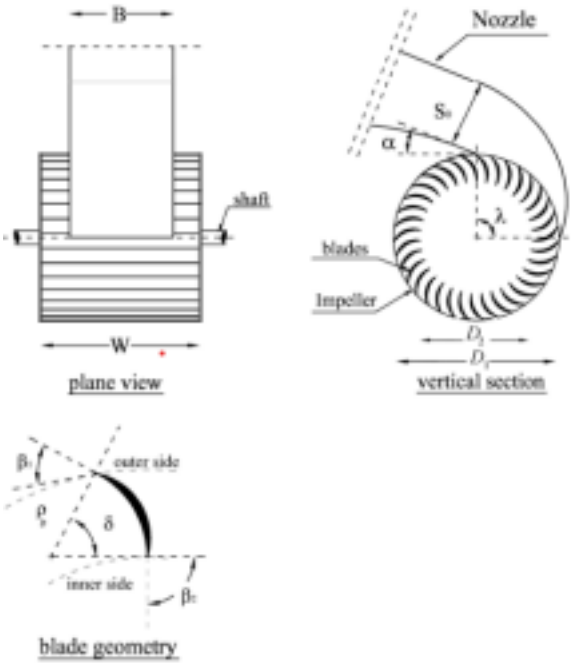

Source: Sammartano et al. (2013)
Fig. 2. Geometrical parameters of the impeller

Table 1. Design parameters of the impeller

Parameter	Value	Description
D1 (mm)	161	Impeller outer perimeter diameter
D2 (mm)	109	Impeller inner perimeter diameter
Nb (-)	35	Number of blades
λ (º)	90	Inlet discharge angle
α (º)	22	Attack angle of the outlet nozzle velocity
$\beta 1$ (º)	38.9	Angle between the blade and the outer perimeter of the impeller
$\beta 2$ (º)	90	Angle between the blade and the inner perimeter of the impeller
ρb (mm)	27.7	Radius of blade
δ (º)	61.5	Central angle of blade
So (mm)	47	Nozzle initial height
B (mm)	93	Nozzle width
K (-)	31.5	Constant in reference [8]
W (mm)	139	Impeller width

Source: Sammartano et al. (2013)

In Table 2, the focus of meshing treatment uses a simple meshing method with the form of hexahedral unstructured mesh with the help of the multizone method. This is to speed up the meshing process. The results of meshing are acceptable because even though using unstructured mesh the average results can be validated with errors below

10%. Other meshing treatments such as boundary layer thickness is not applied because it makes the simulation process to be erroneous due to Courant-Friedrichs-Lewy (CFL) number is changing too significantly during transient simulation. The error can be avoided by decreasing the time step size to be smaller.

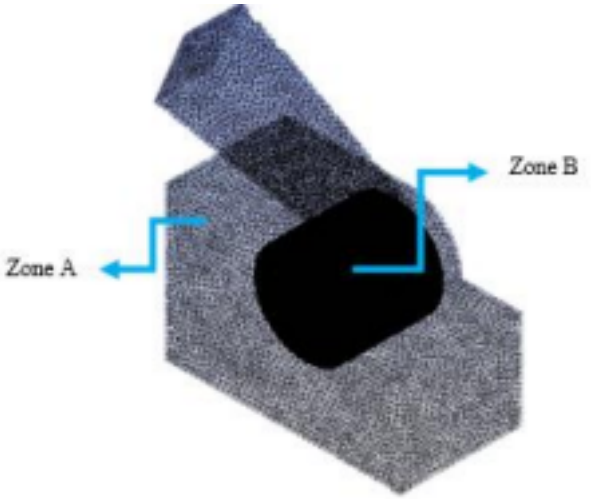

Fig. 3. Physical Domain of simulation

Table 2. General meshing settings

Zone	Meshing Method	Treatments	Remarks
A	Semi structural mesh	Multizone	Setup hexa mapped mesh type
		Body sizing	Element size 5 mm
B	Semi structural mesh	Multizone	Setup hexa mapped mesh type
		Body sizing	Element size 1 mm
	Stuctural O-Grid Mesh	Sweep method	Setup hexa mapped mesh type
		Body sizing	Element size 1 mm
		Body sizing	Element size 2 mm

However, this will be very ineffective in the simulation calculation process. Meanwhile, the unstructured hexahedral mesh is chosen so that during the mesh motion method, the mesh can generate with simulation errors (floating) much lower than the conventional blocking method. The result of meshing can be seen in Figure 4. The detail mesh of the impeller is shown in Figure 5. The quality of the mesh is excellent, in accordance with the standard [15], shown in Table 3.

Mesh independence test is also done by varying zone B using sizing variations of 5 mm, 3 mm, 2.5 mm, 2 mm, 1.5 mm, and 1.25 mm. According to the results of mesh independency in Figure 6, then a size of 1.5 mm is used because at that sizing the simulation results is no longer influenced by the number of grids.

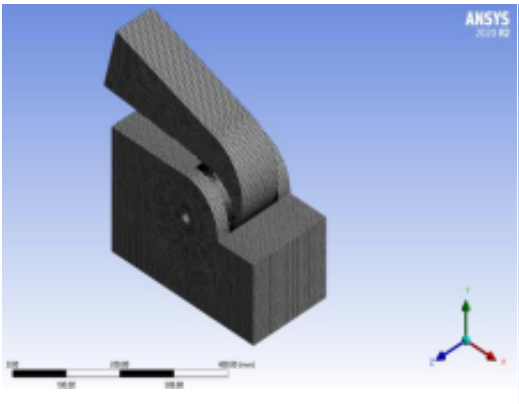

Fig. 4. Mesh result of physical domains

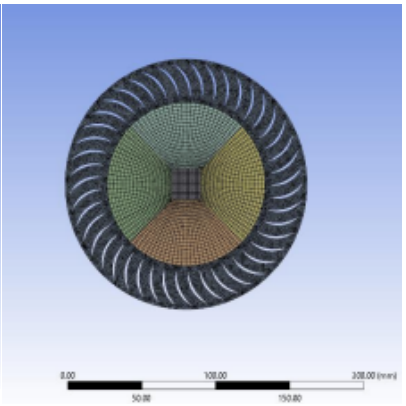

Fig. 5. Mesh of zone B (impeller)

Table 3. Mesh quality

Orthogonal Quality	Min.	0.19288
	Max.	1
	Average	0.97616
	Standard Deviation	5.729e-002
Skewness	Min.	1.3057e-010
	Max.	0.88889
	Average	0.12262
	Standard Deviation	0.12513

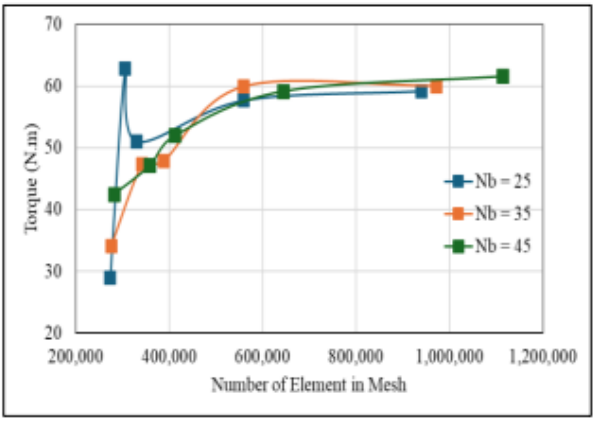

Fig. 6. Mesh independence

Simulations were carried out using commercial CFD code ANSYS Fluent R20.2. Implementing pressure based solver and running in a transient regime. The $k-\omega$ with shear stress transport (SST) turbulence model is selected. The ω-equation has significant advantages near the surface and accurately predicts turbulent length scale in adverse pressure drops. Production Kato Launder and Production Limiter is also

implemented to reduce turbulence production as suggested by literatures to provide a better estimation of the turbine performance compared to other models [14][16].

In the cell zone conditions, non-rotating parts (casing and nozzle) and rotating part (impeller) are defined as water-liquid with mesh motion settings and rotational speed 757 rpm according to the reference design. Then, the calculation is set for 1.5s with time step size 0.001s and maximum iterations of 20, so the total number of iterations is 30,000.

2.2 Data Collective and Validation

Output data taken from the simulations are output torque, velocity and pressure contours. After obtaining the output torque then it is processed to calculate output power. Pressure and velocity contours are used to analyze the behaviours in the system during simulation process. In this case, output power can be calculate using the following formula [4][11][12]:

$$P_{out} = T.\omega \tag{1}$$

$$P_{out} = \frac{2\pi nT}{60} \tag{2}$$

Where P_{out} is the output power measured at the shaft center (watt), T is shaft torque (N.m), ω is angular velocity of turbine (rad/s), n is shaft rotational speed. Then efficiency turbine can be calculate using formula:

$$\eta = \frac{P_{out}}{P_{in}} \times 100\% \tag{3}$$

$$P_{in} = \gamma HQ \tag{4}$$

Where η is turbine efficiency (%), P_{in} is the hydraulic power of the water in the inlet of the turbine (watt), γ is specific weight of water, H is total head (m), Q is flow rate (m^3/s).

It is important to validate the numerical simulation results with available experimental data. This ensures that the simulation model reflects the actual flow behaviours in the field. The validation process in CFD simulation is a critical step to ensure that the numerical model used provides accurate and reliable results. This process involves quantifying input uncertainty and physical model uncertainty [17]. The validation process can be done by comparing simulation results to experimental results. In this study, the data is validated with experiment study by Sammartano et al. (2016). It is expected to produce result simulations with an error below 10% so that the simulation results can be said to be valid.

3 RESULT AND DISCUSSION

3.1 Output Data and Efficiency

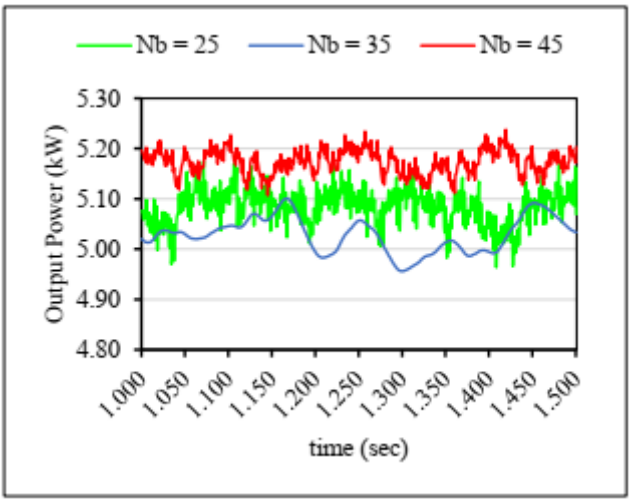

Fig. 7. Output Power

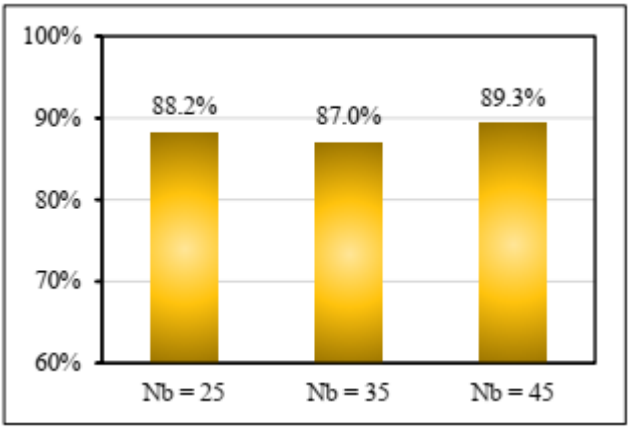

Fig. 8. Efficiency

The torque data obtained from the simulation results is used to calculate power. Thus the efficiency of the turbine can be calculated as well. Based on the simulation result, the maximum output power obtained using 25, 35 and 45 runner blades are 5.17 kW, 5.10 kW and 5.24 kW, respectively, shown in Figure 7. In terms of efficiency, the efficiency increased by 2.3% when number of runner blades increased from 35 to 45. Interestingly, the efficiency also increased by 1.2% when number of runner blades decreased from 35 to 25, shown in Figure 8. Meanwhile, to validate the simulation

results, a comparison of efficiency with the experimental data was conducted, shown in Figure 9. As a result, there is still 6.4% error in the simulation compared to the experimental test using 35 runner blades, which is still acceptable (below 10%) and thus validates the simulation results.

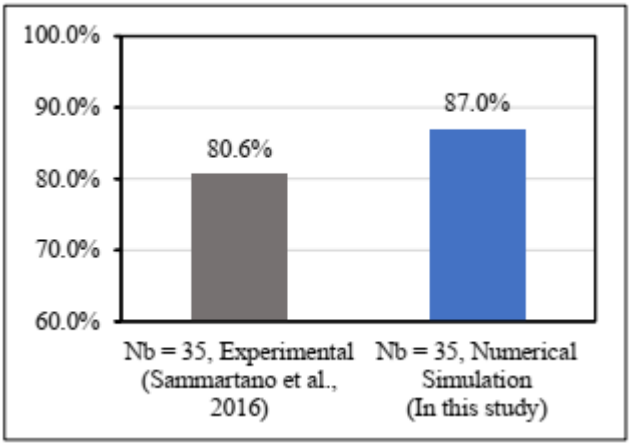

Fig. 9. Validation, simulation compared to experimental test

3.2 Effect of number of runner blades variation

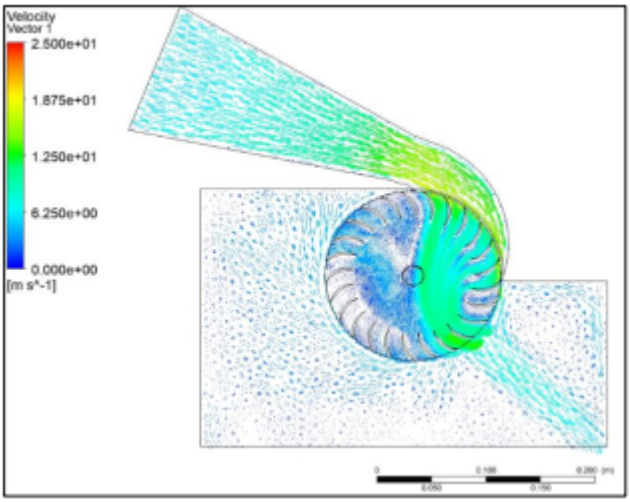

Fig. 10. Velocity Contour, Nb = 25

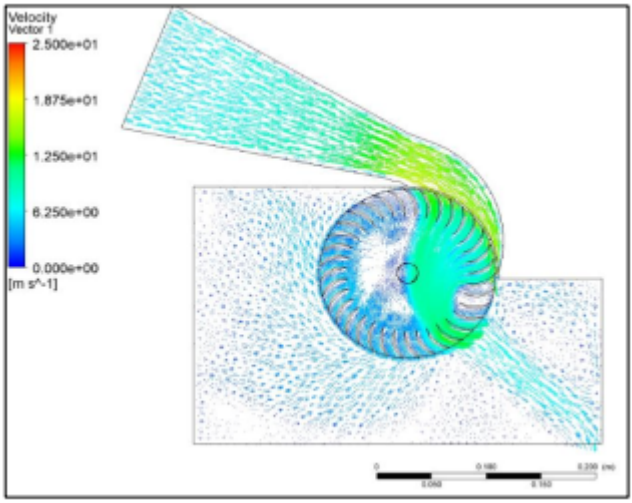

Fig. 11. Velocity Contour, Nb = 35

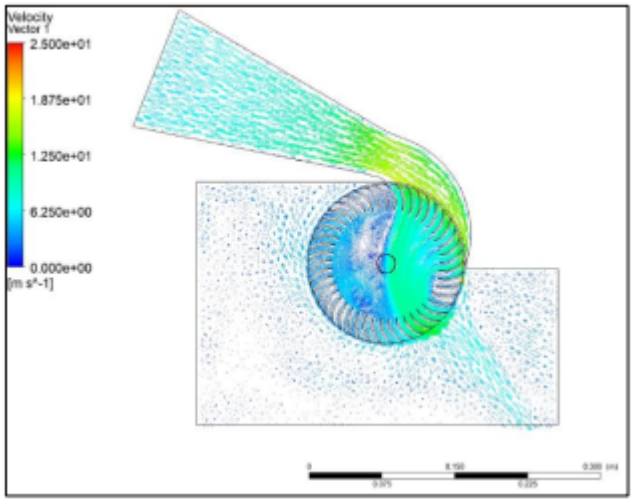

Fig. 12. Velocity Contour, Nb = 45

The velocity contour analysis reveals a near-identical profile, yet a notable discrepancy exists in the direction of discharge angle. When the blade is in a more elevated position, the discharge angle exhibits a greater downward inclination. Conversely, when the blade is in a lower position, the discharge angle displays a reduced downward tilt, shown in Figure 10, Figure 11 and Figure 12. In addition to influencing the direction of the many blades, this discharge angle variation can also serve to quantify the kinetic energy absorbed, ultimately contributing to an enhanced turbine rotational motion.

A notable distinction can be observed in the pressure contour, where the inlet pressure to the turbine is considerably higher in blade 25 compared to blades 35 and

45. This suggests that the absorption of inlet pressure has not been optimized. While blade 35 is almost identical to blade 45, the pressure on the centre side of the turbine decreases more significantly in blade 45 than in blade 35, shown in Figure 13, Figure 14 and Figure 15. Consequently, blade 45 exhibits the highest efficiency compared to the other blades, as the pressure is converted into kinetic energy within the turbine.

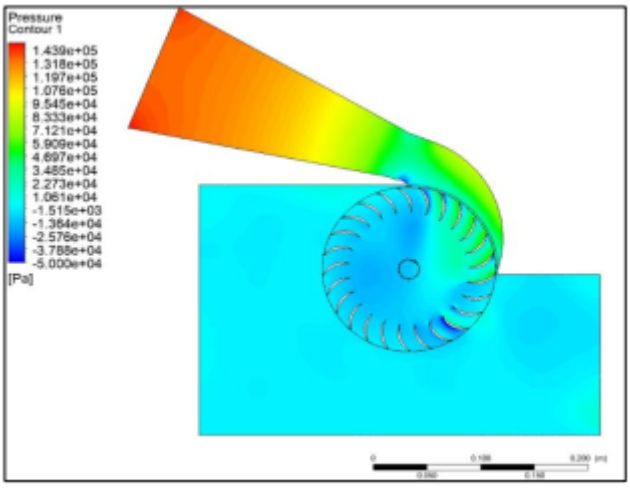

Fig. 13. Pressure Contour, Nb = 25

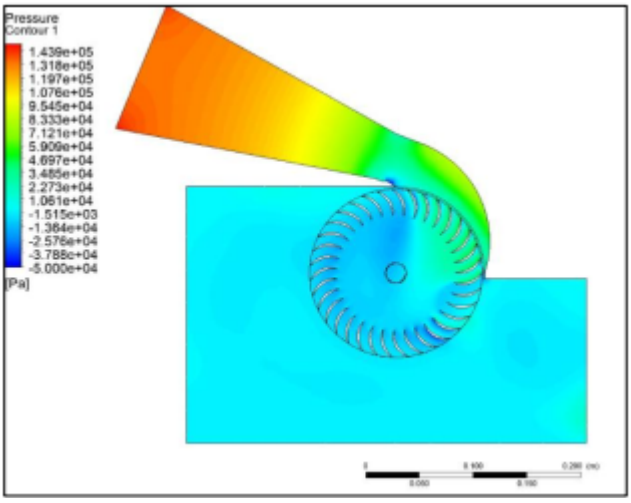

Fig. 14. Pressure Contour, Nb = 35

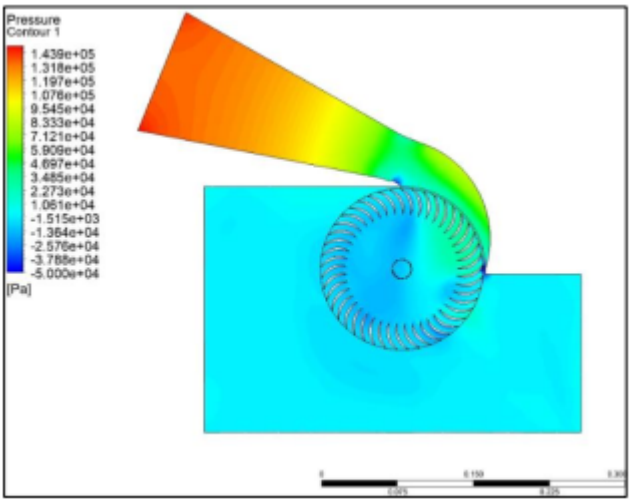

Fig. 15. Pressure Contour, Nb = 45

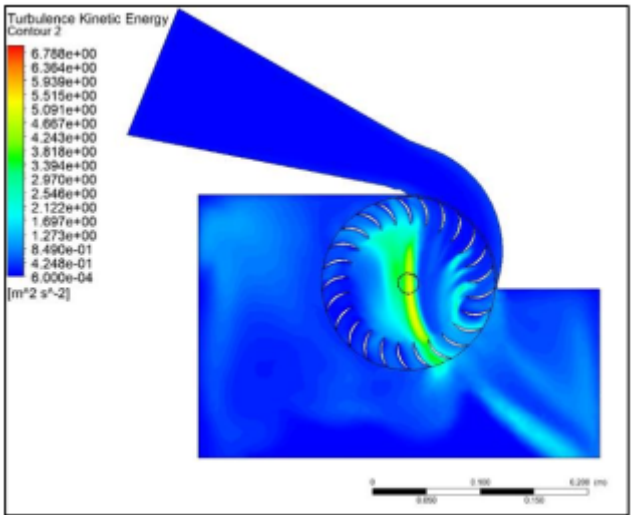

Fig. 16. Turbulent Kinetic Energy, Nb = 25

In the performance section, it was determined that blade 35 exhibited reduced efficiency during the test. To identify the underlying cause, turbulence contours were employed. It was ascertained that within blade 35, turbulence occurred with a considerable amount of turbulent kinetic energy in the central flow of the turbine shown in Figure 16, Figure 17 and Figure 18. This resulted in a lower efficiency than blades 45 and 25, due to the presence of losses within the central path area of the turbine.

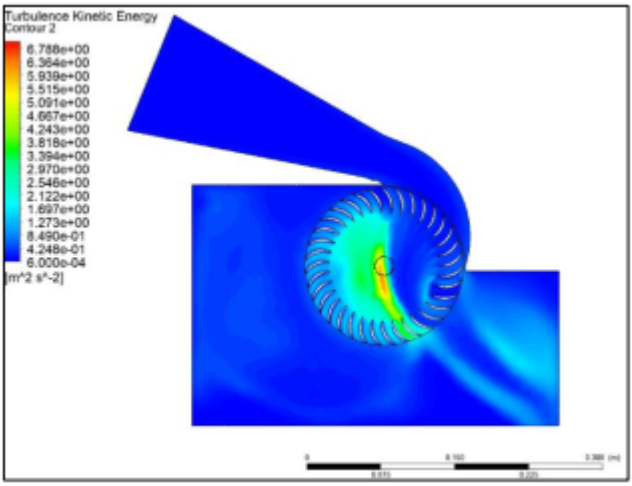

Fig. 17. Turbulent Kinetic Energy, Nb = 35

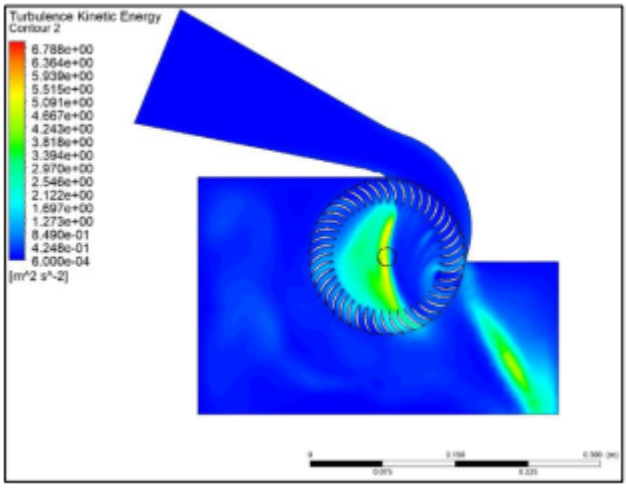

Fig. 18. Turbulent Kinetic Energy, Nb = 45

4 CONCLUSIONS

The number of runner blades has an impact on the performance of the cross-flow tu bine, with variations in this parameter influencing the turbine efficiency. The results of the simulations presented in this study indicate that the maximum efficiency obtained using 25, 35 and 45 runner blades are 88.2%, 87%, 89.3% respectively. Thus, it can be concluded that cross-flow turbine with 45 runner blades provided the highest efficiency. This is due to the absorption of potential and kinetic energy into rotational motion. Furthermore, the turbulent kinetic energy in the impeller section is also lower,

indicating that few losses occur in the system. Nevertheless, there is still an error of 6.4% compared to the experimental study that requires optimisation in the next study.

References

1. Irena. The Changing Role of Hydropower: Challenges and Opportunities. International Renewable Energy Agency, Abu Dhabi (2023)
2. Irena. Renewable capacity statistics 2022. International Renewable Energy Agency, Abu Dhabi (2022b)
3. Irena. World energy transitions outlook 2022: 1.5°C Pathway. International Renewable Energy Agency, Abu Dhabi (2022a)
4. Anand, R. S., Jawahar, C. P., Bellos, E., & Malmquist, A. A comprehensive review on Crossflow turbine for hydropower applications. In Ocean Engineering (Vol. 240). Elsevier Ltd (2021)
5. Williams, A., & Porter, S. Comparison of hydropower options for developing countries with regard to the environmental, social and economic aspects. In: International Conference on Renewable Energy for Developing Countries, USA (2006).
6. Nasir, B. A. Design considerations of micro hydro-electric power plant. Energy Procedia, 50, 19–29 (2014).
7. Sammartano, V., Morreale, G., Sinagra, M., Collura, A., & Tucciarelli, T. Experimental study of Cross-Flow micro-turbines for aqueduct energy recovery. Procedia Engineering, 89, 540–547 (2014).
8. Nasir, B. A. Design of High Efficiency Cross-Flow Turbine for Hydro-Power Plant. In International Journal of Engineering and Advanced Technology (IJEAT) (2013).
9. Elbatran, A. H., Yaakob, O. B., Ahmed, Y. M., & Shabara, H. M. Operation, performance and economic analysis of low head micro-hydropower turbines for rural and remote areas: A review. In Renewable and Sustainable Energy Reviews (Vol. 43, pp. 40–50). Elsevier Ltd (2015).
10. Montanari, R. Criteria for the economic planning of a low power hydroelectric plant. Renewable Energy, 28(13), 2129–2145 (2003).
11. Sammartano, V., Aricò, C., Carravetta, A., Fecarotta, O., & Tucciarelli, T. Banki Michell optimal design by computational fluid dynamics testing and hydrodynamic analysis. Energies, 6(5), 2362–2385 (2013).
12. Desai, V. R., & Aziz, N. I. An Experimental Investigation of Cross-Flow Turbine Efficiency (1994).
13. Sinagra dkk. Cross-Flow turbine design for variable operating conditions. Procedia Engineering, 70, 1539-1548 (2014)
14. Sammartano, V., Morreale, G., Sinagra, M., Tucciarelli, T. Experimental and Numerical Analysis of a Cross-Flow Turbine. Journal of Hydraulic Engineering, 142(1) (2016).
15. Ansys Inc. Introduction to ANSYS Meshing (2015)
16. Ansys Inc. ANSYS Fluent Tutorial Guide (2017)
17. Versteeg, H. K., & Malalasekera, W. An Introduction to Computational Fluid Dynamics Second Edition (2007)